# Interlocking Folded Plate – Integral Mechanical Attachment for Structural Wood Panels

*by*

**C. Robeller and Y. Weinand**

*Reprinted from*

INTERNATIONAL JOURNAL OF
SPACE STRUCTURES
Volume 30 · Number 2 · 2015

MULTI-SCIENCE PUBLISHING CO. LTD.
5 Wates Way, Brentwood, Essex CM15 9TB, United Kingdom

Figure 12. Folded-plate arch prototype built from 12 mm birch plywood (9-layer, I-I-I-I-I). Assembled without adhesive bonding or metal fasteners. Span 1.65m, self-weight 9.8 kg.

assembly of long edges may be more difficult but can be simplified with a modified joint geometry. It is important to know the approximate direction of insertion for each part, as this is not easily visible through the joint geometry. Deformations of the arch during the assembly should be minimised. We have assembled this first prototype lying on the side. However larger assemblies may require temporary punctual supports. Although the in-plane dimensional stability of the Kerto-Q panels is very high, panels may be slightly warped and some force may be necessary during assembly. While we have simply used a rubber mallet, more advanced techniques could be applied.

To understand the mechanical behaviour of the built prototype, we have applied a vertical load at mid-span of the arch and measured the vertical deflection at the same point. The total load of 821 N was applied in two identical load cycles consisting of four loading/unloading sub-cycles. First, a vertical load of 117 N was applied in seven steps, after which the load of the last four steps was removed. The loading and unloading of the last four steps was repeated three more times, after which the complete load was removed and the residual deflection was measured. (Figure 13).

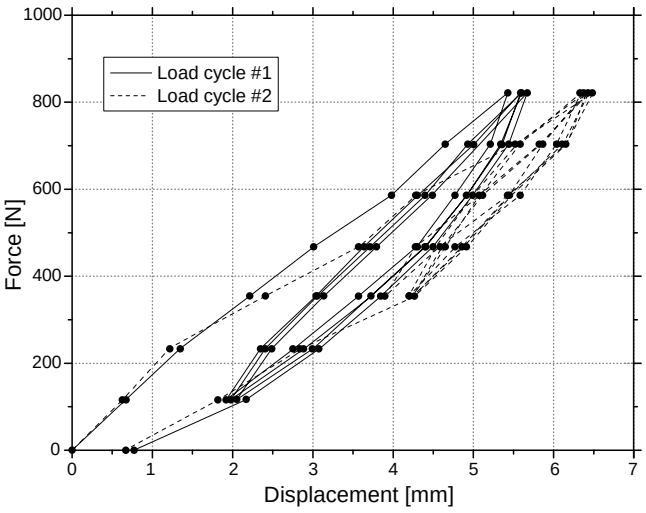


Figure 13. Series of 3-point flexural tests on the small scale interlocking arch prototype built from Metsawood 12 mm birch plywood panels.

Under a vertical load equal to the archs dead weight of 9.8kg (98 N), the deflection measured at mid-span was 2 mm. From this we obtain a span-to-deflection-ratio of *L*/750 and the arch's structural efficiency which reaches 8.6 when loaded with 821 N (ratio of the maximal load over the dead weight of the arch).

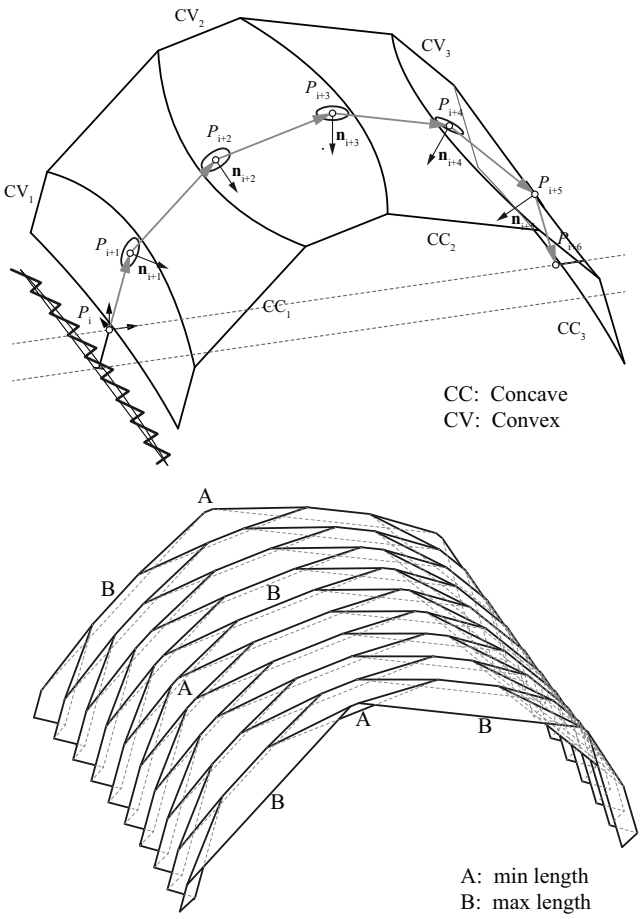


Figure 14. Doubly-curved folded-plate: The radius ($R = 17m$) of the transversal curvature is determined by the folded plates maximum amplitude $h$ [2], which is inversely proportional to the number of segments $m$ of the cross-section polyline (grey). We obtain this polyline from a circular arc divided into segments of equal length. The interior angle $\gamma = ((m - 2) * 180) - m$ of this polyline is proportional to all fold angles $\varphi$. The geometry of our prototype was fabrication-constrained to a maximum component length $B \leq 2{:}5m$.

## 3. INTERLOCKING SHELL PROTOTYPE

### 3.1. Automatic Geometry Processing

Using the RhinoPython application programming interface, we have developed a computational tool which lets us instantly generate both the geometry of the individual components and the machine G-Code required for fabrication. The tool processes arbitrary polygon meshes, and generates 1DOF joints for all non-naked edges where the fold angle $\varphi$ is larger than $\varphi_{min}$ and smaller than $\varphi_{max}$ shown in figure 5 (non-smooth meshes). It also requires an input of edge identifier tuples identifying those edges which must be jointed simultaneously, as well as the thickness of the LVL panels. Exploiting this geometrical freedom, we have tested our computational tool on the design of a folded plate shell prototype with an alternating convex-concave transversal curvature. The shell spans over 3 m at a thickness of 21 mm, using Kerto-Q structural grade LVL panels (7-layer, I-III-I). (Figure 14).

Comparing this doubly-curved folded plate with a straight extrusion (as tested by H. Buri [2]), it can be concluded that the slight double-curvature proves to be very beneficial when it comes to global deflections, for example those caused by wind loads. Deflections for the doubly-curved shell geometry in the vertical direction are up to 39% smaller and up to 13% smaller in the lateral direction than the ones for the straight extrusion one.

### 3.2. Assembly

Due to the different assembly directions of its 239 joints, the 107 components components in our prototype interlock with one another, similar to a *Burr Puzzle* [22]. Figure 15 shows a part of a so called *non-directional*

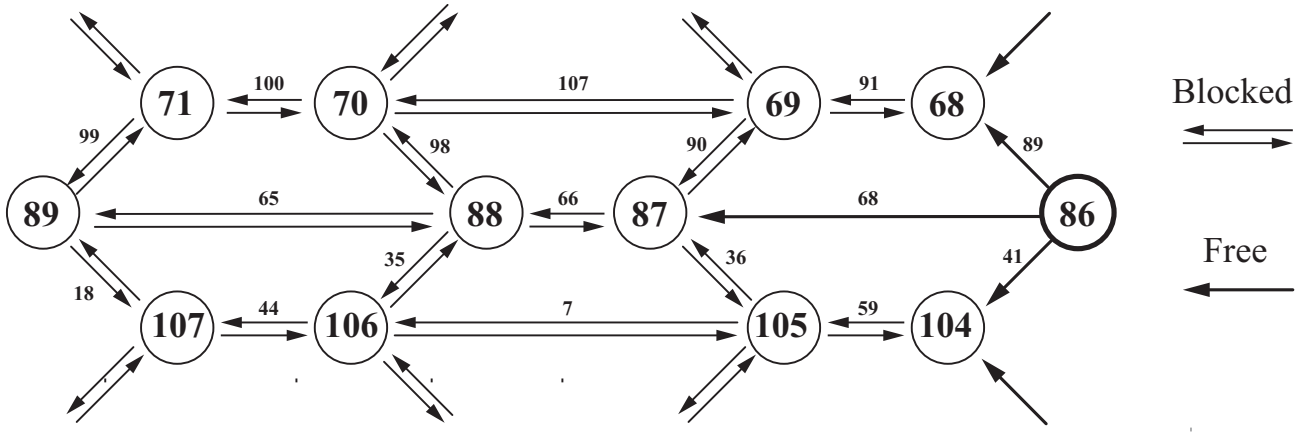


Figure 15. Partial connectivity, assembly and blocking graph of the folded plate shell prototype. (Left-to-right assembly) Large numbers represent mesh faces, small numbers represent mesh edges.

*blocking graph* (NDBG), which was inroduced by Wilson and Latombe [21].

In such a graph, single arrows indicate that parts can be removed from the assembly. Two opposite arrows between parts indicate that the connection is blocked. In order to remove blocked parts, the blocking parts must be removed first. Our graph illustrates a left-to-right assembly. On the right side, part number 86 is being inserted. It connects to three other plates and blocks all other parts in the graph. In such a configuration, the final part remains removable, it is called the *key*.

Figure 16 shows the parts from figure 15 in 3D, demonstrating how the component based on mesh face $F_{86}$ is being inserted. Its three edgewise joints $E_{41}$, $E_{68}$ and $E_{89}$ must be assembled simultaneously. The three assembly vectors of the edges and $\overrightarrow{v_{41}}$, $\overrightarrow{v_{68}}$ and $\overrightarrow{v_{89}}$ have been rotated to be parallel. The same applies for the

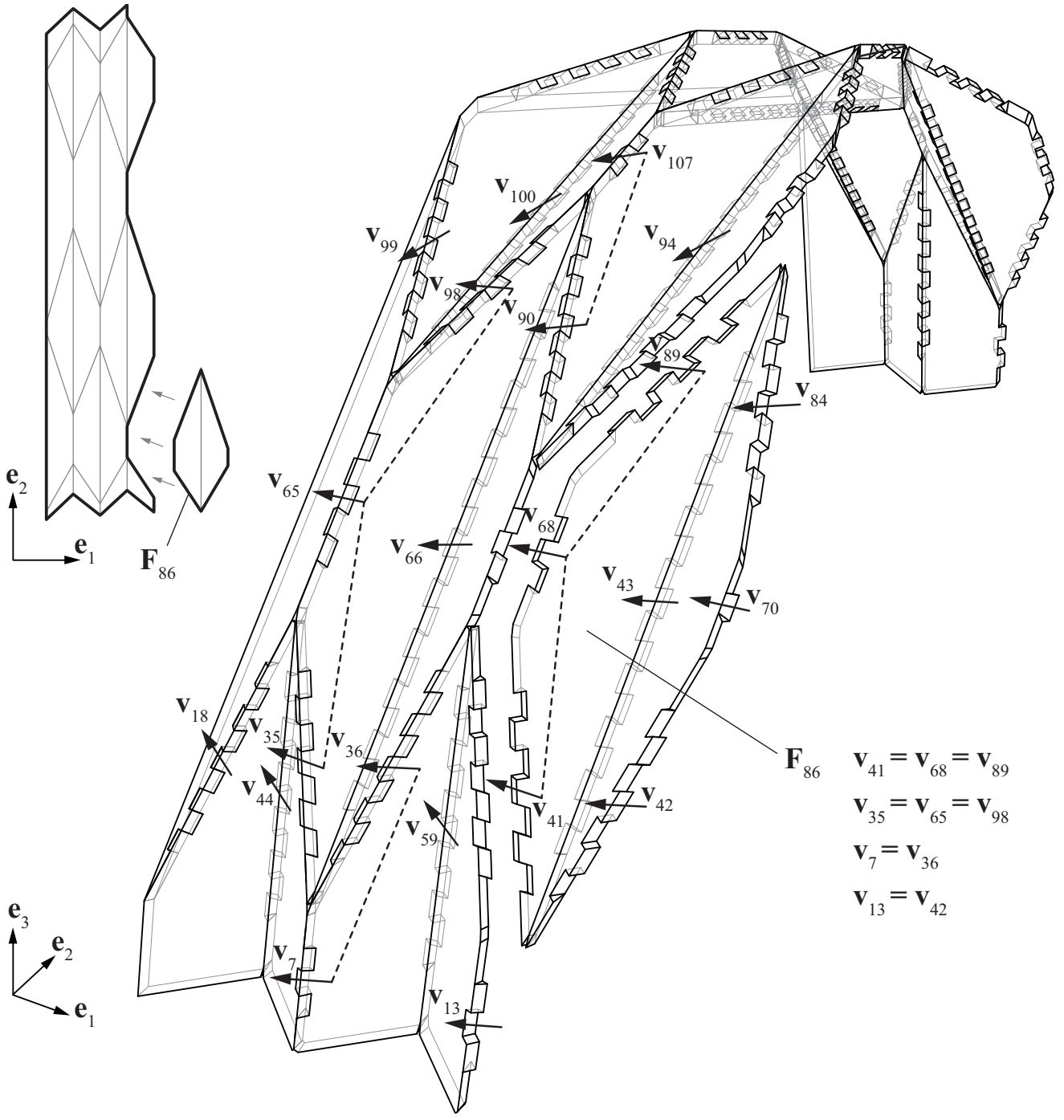


Figure 16. Left-to-right assembly of the Interlocking folded plate shell prototype. Built from Kerto-Q structural grade LVL panels (7-layer, I-III-I)).

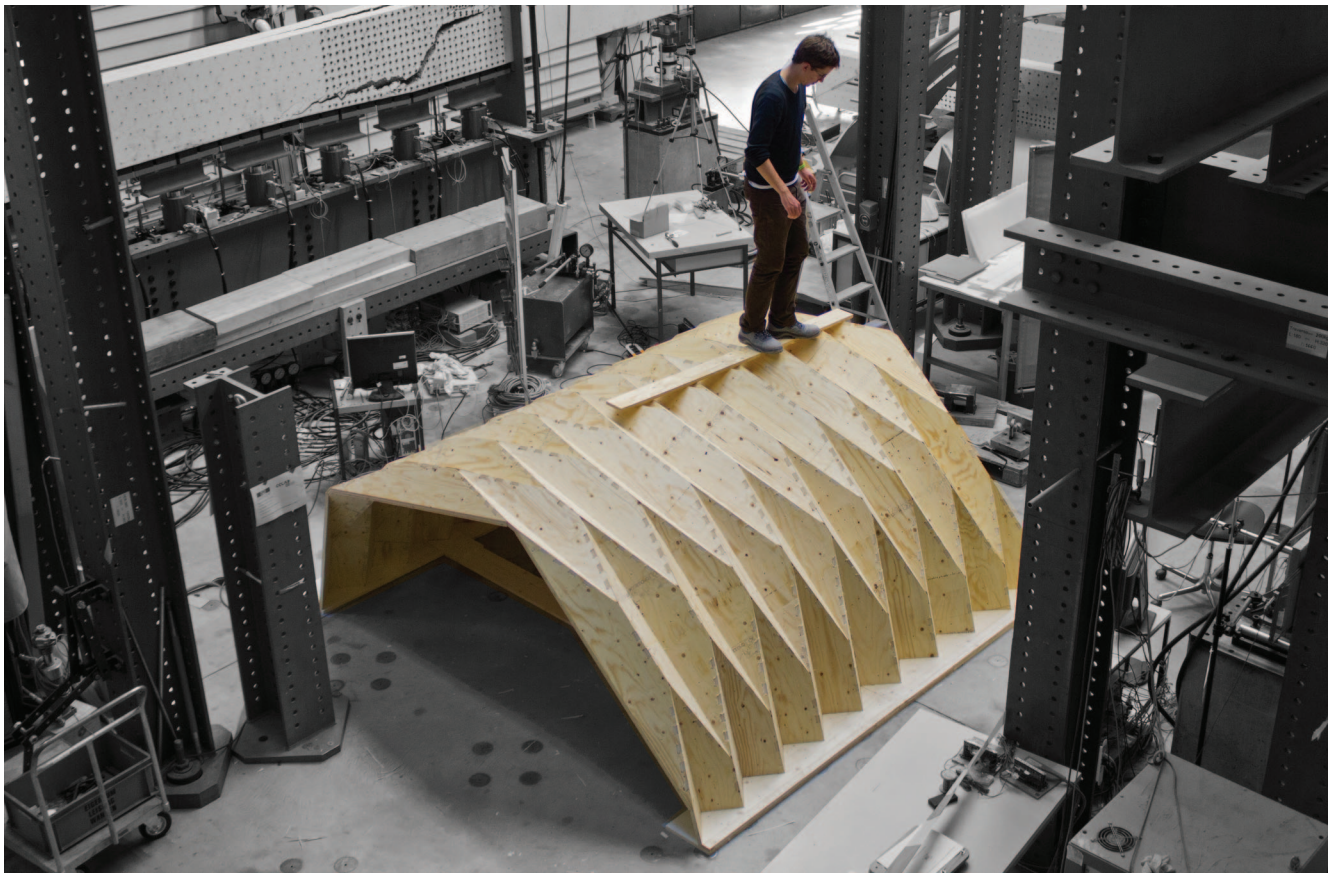

Figure 17. Folded-plate shell prototype, built from 21 mm LVL panels. With a self-weight of 192 kg, the prototype with a span of 3 m was tested with a line-load up to 45 kN.

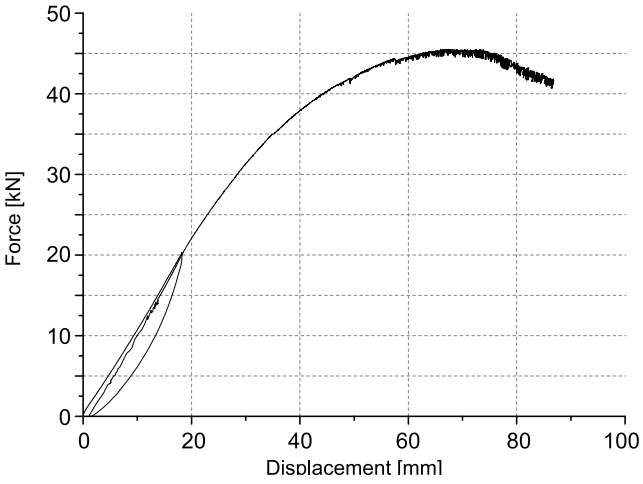


Figure 18. Load-displacement curve of the shell prototype. A longitudinal line load was introduced along the top of the shell. Vertical displacement was measured at the center point.

adjacent edges on the left side of the faces $F_{67}$, $F_{69}$, $F_{88}$, $F_{103}$ and $F_{105}$ (see figure 15). Within the rotation window of the edge, we can freely rotate $\vec{v}$ for these edges (the greater the angle between $\vec{v}$ and the main direction of traction $e_1$, the better).

### 3.3. Completed Shell Prototype and Load Test

Figure 17 shows the completed folded plate prototype, with a span of 3 m and a shell thickness of 21 mm. Boundary conditions that restrain displacements of the supports in every direction, but allow rotations, were applied on both sides. A longitudinal line load was introduced along the top of the shell and vertical displacement was measured at center point. (Figure 18).

The prototype structure was also modelled in FE analysis software (Abaqus) and loaded in the same way. The plates were modelled using shell elements, where the mid-surface is used to represent the 3D plate and transverse shearing strains are neglected. Connections between the plates were considered as completely rigid in order to obtain minimal displacements of the structure. By comparing the displacements of the structure with infinitely stiff joints with the ones measured on the prototype, we obtained information about the actual semi-rigidity of the joints. The results obtained from the testing of the large scale prototype showed that the load of 25 kN, that corresponds to the proportional limit of

the load-displacement curve, causes a vertical displacement of 23 mm. In the FE model, the load applied in the same manner caused a vertical displacement of 2.6 mm.

## 4. CONCLUSION

A timber folded plate shell combines the structural advantages of timber panels with the efficiency of folded plates. However, in such discrete element assemblies, a large amount of semi-rigid joints must provide sufficient support for the adjacent plates in oder to ensure an efficient load-bearing system. This remains a challenge with much potential for improvements [5].

Integrated edgewise joints present an interesting addition and an alternative to state-of-the-art connectors: Compared to adhesive bonding, such joints can be assembled rapidly on site. Also, compared to costly metal plates and fasteners, which are typically required in large quantities [14], the fabrication of integrated joints is not more expensive. The replacement or reduction of metal fasteners with an integrated mono-material connection includes advantages such as improved aesthetics, ease-of recycling or a homogenous thermal conductivity of the parts, which can reduce condensation and decay [4]. Another particular advantage is the possibility to join thin panels: The current technical approval for the Kerto-Q panels does not permit screwed joints on panels with a thickness of less than 60 mm [3].

Recent experimental projects, which we introduced in chapter 1, have already demonstrated first applications of integrated edgewise joints for timber panels. This paper followed up on these projects, examining the particular advantages, potential and challenges of 1DOF joints for timber folded plate shells. We have demonstrated how this joint geometry helps resisting the forces which occur in such structures. In addition to the load-bearing connector features, the joints provide locator features, which allow for precise positioning and alignment of the parts through the joint geometry. This improves both accuracy and ease of assembly. Furthermore, we have presented a solution for the simultaneous assembly of multiple edges per panel, which is essential for the application of 1DOF joints in a folded plate shell structure. The per edge "rotation window" introduced in section 1.3 integrates the joint constraints related to assembly and fabrication. It can be processed algorithmically and gives instant feedback on whether or not a set of non-parallel edges can be jointed simultaneously. This provides a tool for the exploration of a variety of alternative folded plate shell geometries.

The prototypes presented in this paper already suggest possible patterns and demonstrate the reciprocal relationship between the geometry of the plates and the joints. Two built structures allowed us to test and verify the proposed methods for fabrication and assembly while providing valuable information about the load-bearing capacity of the integrated joints.

For the application in a large-scale building structure, further research is required to determine if the integrated joints can replace additional connectors entirely or reduce their amount. A possible combination of integrated joints with additional metal fasteners has been demonstrated recently in the LaGa Exhibition Hall [10]. Another possibility would be a combination of the 1DOF joints with integrated elastic interlocks [17].

## 5. ACKNOWLEDGMENTS

We would like to thank Andrea Stitic and Paul Mayencourt for their support with the finite element models and load testing of the prototypes, as well as Gabriel Tschanz and Francois Perrin for assisting with the fabrication and assembly of prototypes. We also thank Jouni Hakkarainen and the Metsa Group for the supply of information and materials.

## REFERENCES

[1] B.S. Benjamin and Z.S. Makowski. The analysis of folded-plate structures in plastics. In *Proceedings of a conference held in London*, pages 149–163. Pergamon Press, London, 1965.

[2] Hani Buri and Yves Weinand. BSP Visionen - Faltwerkkonstruktionen aus BSP-Elementen. In *Grazer Holzbau-Fachtage*, 2006.

[3] DIBt. *Allgemeine bauaufsichtliche Zulassung Kerto-Q Z-9.1-100, Paragraph 4.2 and Attachment No. 7, Table 5*. Deutsches Institut fur Bautechnik, 2011.

[4] Wolfram Graubner. *Holzverbindungen, Gegenüberstellung von Holzverbindungen Holz in Holz und mit Metallteilen*. Deutsche Verlags-Anstalt Stuttgart, 1986.

[5] Benjamin Hahn. Analyse und beschreibung eines räumlichen tragwerks aus massivholz-platten. Master's thesis, EPFL, Lausanne, 2009. Master Thesis.

[6] HESS. Hess limitless, 2014. http://www.hess-timber.com/de/produkte/.

[7] Hundegger. Hans Hundegger Maschinenbau GmbH, Hawangen, Germany, 2014. http://www.hundegger.de/en/machine-building/company/our-history.html.

[8] Peter Koch. *Wood Machining Processes*. Wood Processing. Carl Hanser Verlag GmbH and Co. KG, 1964.

[9] Tetsuya Kōndo. *Dento kanehozo kumitsugi: Sekkei to seisaku no jissai*. LLP Gijutsushi Shuppankai, Tokyo: Seiunsha, 2007.

[10] Oliver Krieg, Tobias Schwinn, Achim Menges, Jian-Min Li, Jan Knippers, Annette Schmitt and Volker Schwieger.

Computational integration of robotic fabrication, architectural geometry and structural design for biomimetic lightweight timber plate shells. In *Advances in Architectural Geometry 2014*. Springer Verlag, 2014.

[11] Oliver David Krieg, Zachary Christian, David Correa, Achim Menges, Steffen Reichert, Katja Rinderspacher and Tobias Schwinn. Hygroskin: Meteorosensitive pavilion. In *Fabricate 2014 Conference Zurich*, pages 272–279, 2014.

[12] Riccardo la Magna et al. From nature to fabrication: Biomimetic design principles for the production of complex spatial structures. *International Journal of Spatial Structures*, Vol. 28 No. 1:27–39, 2013.

[13] Robert W. Messler. *Integral Mechanical Attachment: A Resurgence of the Oldest Method of Joining*. Butterworth Heinemann, 2006.

[14] Helmuth Neuhaus. *DIN EN 1995 (Eurocode 5) - Design of timber structures*. DIN Deutsches Institut fur Normung e. V., 2004.

[15] Purbond. *National Technical Approval Z-9.1-711/Single-component polyurethane adhesive for the manufacture of engineered wood products*. Deutsches Institut für Bautechnik, 2011.

[16] Christopher Robeller. *Integral Mechanical Attachment for Timber Folded Plate Structures*. PhD thesis, ENAC, Lausanne, 2015.

[17] Christopher Robeller, Paul Mayencourt and Yves Weinand. Snap-fit joints: Integrated mechanical attachment of structural timber panels. In *Proceedings of the 34th International Conference of the Association of Computer-aided Design in Architecture ACADIA, Los Angeles, USA*. Riverside Architectural Press, 2014.

[18] Christopher Robeller, SeyedSina Nabaei and Yves Weinand. Design and fabrication of robot-manufactured joints for a curved-folded thin-shell structure made from clt. In Wes McGee and Monica Ponce de Leon, editors, *Robotic Fabrication in Architecture, Art and Design 2014*, pages 67–81. Springer International Publishing, 2014.

[19] Regina Schineis. Gefalteter Klangkoerper Musikprobensaal Thannhausen/Thannhausen Rehearsal Room. In *10. Internationales Holzbau Forum (IHF), Garmisch-Partenkirchen*, 2004.

[20] Vaclav Sebera and Milan Simek. Finite element analysis of dovetail joint made with the use of cnc technology. *Acta Universitatis Agriculturae Et Silviculturae Mendelianae Brunensis*, Volume LVIII:321–328, 2010.

[21] Randall H. Wilson and Jean-Claude Latombe. Geometric reasoning about mechanical assembly. *Artificial Intelligence*, 71(2):371–396, 1994.

[22] Edwin Wyatt. *Puzzles in Wood*. Bruce Publishing Co., 1928.